Cancer Cell, Volume *14*

Supplemental Data

Article

A Molecule Targeting VHL-Deficient

Renal Cell Carcinoma that Induces Autophagy

Sandra Turcotte, Denise A. Chan, Patrick D. Sutphin, Michael P. Hay, William A. Denny, and Amato J. Giaccia

Table S1. Analog Library

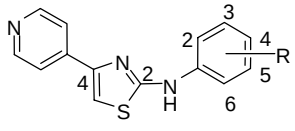

Scheme 1

		IC_{50} (μM)		
Name	**R**	**RCC4**	**RCC4/VHL**	**Ratio**
STF-62247	3-Me	0.625	16	25.6
30602	H	7.5	ND	ND
30603	4-Me	2.5	50	20
30644	4-OMe	15.5	40	2.58
30651	3-OMe	3	ND	ND
30654	3-Cl	3	15	5
30670	3-CF_3	ND	ND	ND
30671	4-Cl	38	ND	ND
30709	4-F	5	ND	ND
30713	3,4-diCl	13.5	ND	ND
31181	3,4-diOMe	20	40	2
31184	4-OH	5.5	80	14.54
31185	3-OH	20	ND	ND
31186	3,4-OCH_2O	ND	ND	ND
31187	3,4-$(CH_2)_3$-	1.75	20	11.43
31258	3-OH, 4-Me	12	56	4.67
31270	3-Me, 4-OH	70	160	2.29
31274	4-$(CH_2)_2OH$	5	80	16
31283	4-$(CH_2)_3NMe_2$	50	60	1.2
31289	4-$O(CH_2)_2NMe_2$	60	75	1.25

The compounds were conveniently prepared using a Hantzsch thiazole synthesis (Scheme 1), where 4-pyridyl α-bromoketones were condensed with variously substituted arylthioureas to give the compounds (manuscript in preparation). IC_{50} was evaluated by XTT assay in RCC4 and RCC4/VHL cells. Ratio is the relative from the IC_{50} in RCC4/VHL cells/IC_{50} in RCC4 cells.

Table S2. Yeast Screen in Response to STF-62247

ORF	Gene	Human Homolog	Description
YPL170W	DAP1	PGRMC1	Heme-binding protein involved in regulation of cytochrome P450 protein Erg11p; damage response protein, related to mammalian membrane progesterone receptors; mutations lead to defects in telomeres, mitochondria, and sterol synthesis
YHR073W	OSH3	OSBPL3	Member of an oxysterol-binding protein family with seven members in S. cerevisiae; family members have overlapping, redundant functions in sterol metabolism and collectively perform a function essential for viability
YLR170C	APS1	LOC653653	Small subunit of the clathrin-associated adaptor complex AP-1, which is involved in protein sorting at the trans-Golgi network; homolog of the sigma subunit of the mammalian clathrin AP-1 complex
YAL026C	DRS2	ATP8A2	Aminophospholipid translocase (flippase) that maintains membrane lipid asymmetry in post-Golgi secretory vessicles; localizes to the trans-Golgi network; contributes to clathrin-coated vesicle formation and endocytosis; type 4 P-type ATPase
YER031C	YPT31	RAB11A	GTPase of the Ypt/Rab family, involved in the exocytic pathway; mediates intra-Golgi traffic or the budding of post-Golgi vesicles from the trans-Golgi
YPL227C	ALG5	ALG5p/ALG5	UDP-glucose:dolichyl-phosphate glucosyltransferase, involved in asparagine-linked glycosylation in the endoplasmic reticulum
YGR063C	SPT4	SUPT4H1	Protein that forms a complex with Spt5p and mediates both activation and inhibition of transcription elongation, and plays a role in pre-mRNA processing; in addition, Spt4p is involved in kinetochore function and gene silencing
YMR077C	VPS20	CHMP6	Myristoylated subunit of ESCRTIII, the endosomal sorting complex required for transport of transmembrane proteins into the multivesicular body pathway to the lysosomal/vacuolar lumen; cytoplasmic protein recruited to endosomal membranes
YJR102C	VPS25	VPS25	Component of the ESCRT-II complex, which is involved in ubiquitin-dependent sorting of proteins into the endosome
YNL298W	CLA4	PAK2	Cdc42p activated signal transducing kinase of the PAK (p21-activated kinase) family, involved in septin ring assembly and cytokinesis; directly phosphorylates septins Cdc3p and Cdc10p; other yeast PAK family members are Ste20p and Skm1p
YNL325C	Fig4	KIAA0274	Protein required for efficient mating, member of a family of eukaryotic proteins that contain a domain homologous to Sac1p
YBL078C	ATG8	LC3	Biological marker for autophagy

Figure S1

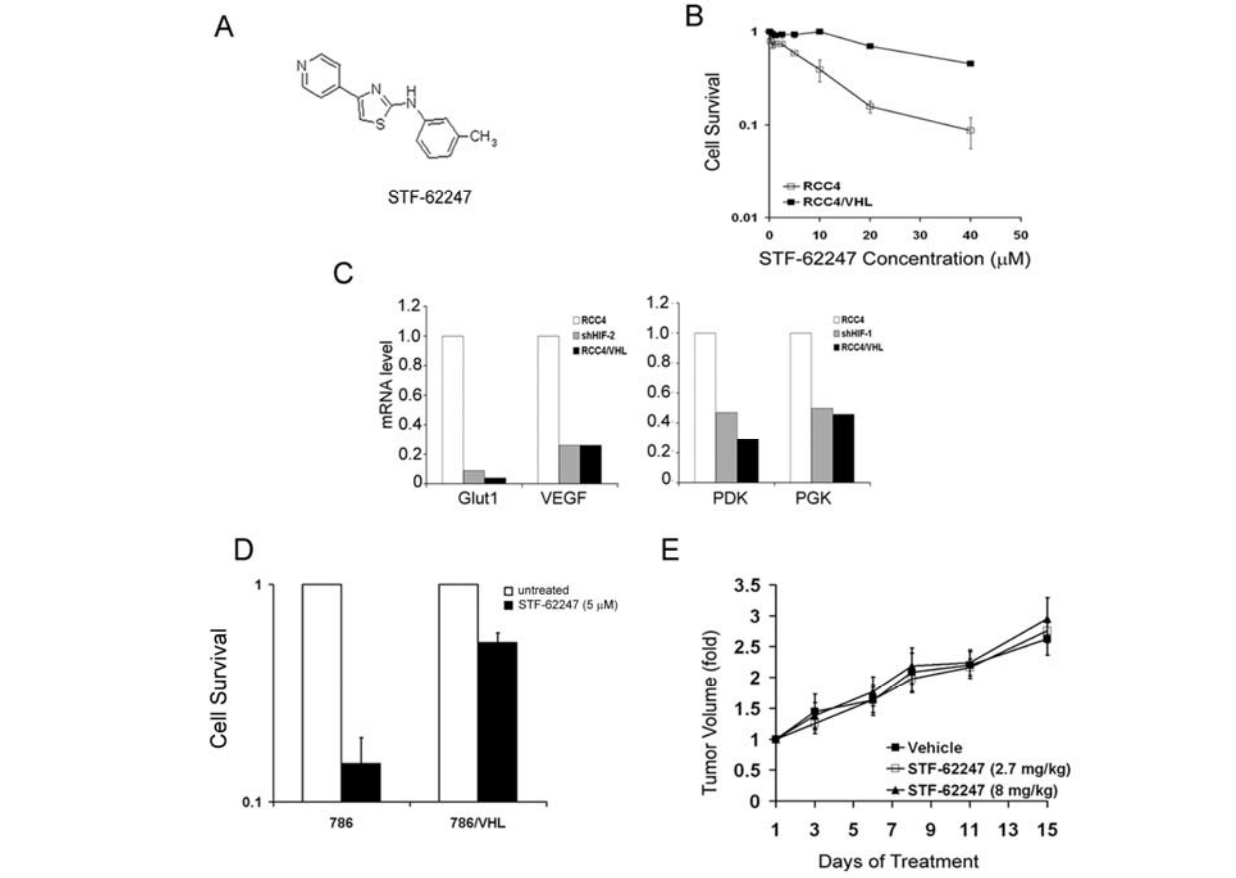
A
STF-62247
B
Cell Survival
RCC4
RCC4/VHL
STF-62247 Concentration (μM)
C
mRNA level
RCC4
shHIF-2
RCC4/VHL
Glut1
VEGF
shHIF-1
PDK
PGK
D
untreated
STF-62247 (5 μM)
Cell Survival
786
786/VHL
E
Tumor Volume (fold)
Vehicle
STF-62247 (2.7 mg/kg)
STF-62247 (8 mg/kg)
Days of Treatment

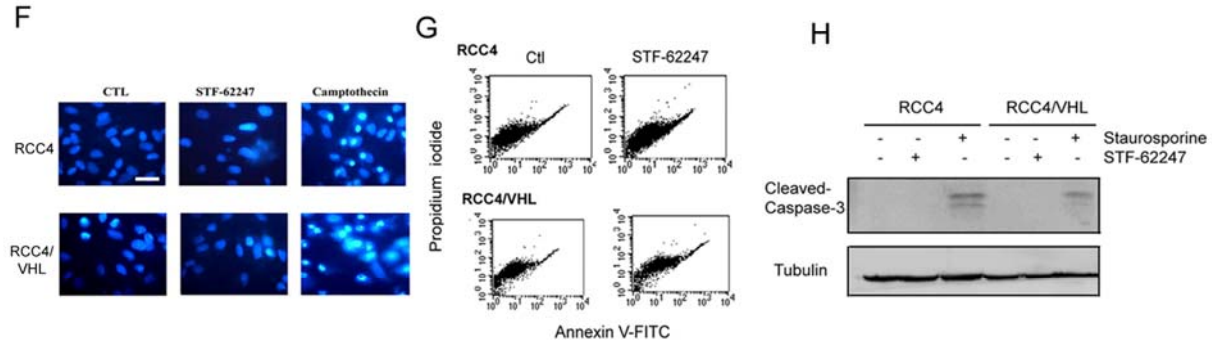
F
CTL
STF-62247
Camptothecin
RCC4
RCC4/
VHL
G
RCC4
Ctl
STF-62247
RCC4/VHL
Propidium iodide
Annexin V-FITC
H
RCC4
RCC4/VHL
Staurosporine
STF-62247
Cleaved-
Caspase-3
Tubulin

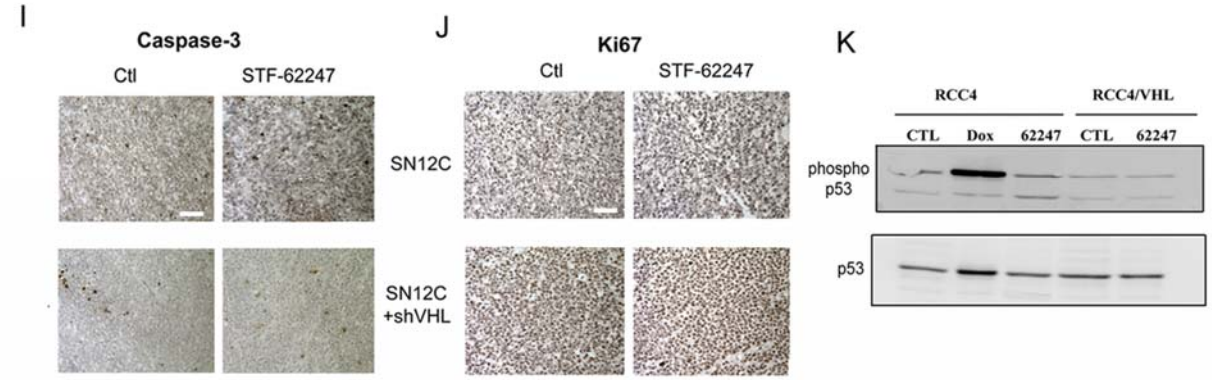
I
Caspase-3
Ctl
STF-62247
SN12C
SN12C
+shVHL
J
Ki67
Ctl
STF-62247
K
RCC4
RCC4/VHL
CTL
Dox
62247
CTL
62247
phospho
p53
p53

Figure S1.

(A) Structure of STF-62247.

(B) XTT assay in RCC4 and RCC4/VHL in presence of STF-62247 (0-40 μM). Each point of the cell survival is calculated by the average of three different experiments in duplicate as the percent of treated versus untreated plate.

(C) qRT-PCR for Glut1, VEGF, PDF and PGK in RCC4 cells with or without HIF-1α, HIF-2α shRNA and in RCC4/VHL.

(D) In vitro clonogenic analysis of 786-O or 786/VHL treated with 5 μM of STF-62247.

(E) SN12C (2-3 x 10^6 cells) were injected into SCID mice. Mice were injected daily by intraperitoneal injection with vehicle, 8 mg/kg or 2.7 mg/kg of STF-62247 in PBS. Tumor growth was measured every 2-3 days after the drug treatment was started.

(F) Hoechst staining in RCC4 and RCC4/VHL cells with 1.25 μM of STF-62247 for 2 days. Camptothecin was used as positive control.

(G) FACS analysis for apoptosis after an annexin V-FITC staining in presence or absence of propidium iodine (PI) in cells after a treatment in same conditions than in C.

(H) Immunoblot for active caspase-3 in RCC4 and RCC4/VHL following treatment with 1.25 μM of STF-62247 for 24 hours. Staurosporine was used as positive control (0.2 μM for 24 hours).

(I and J) Immunostaining of caspase-3 and Ki67 respectively in SN12C and SN12C-VHL shRNA tumor samples untreated or treated with 30 μM of STF-62247.

(K) Immunoblot for p53 and phospho-Ser15 p53 in RCC4 and RCC4/VHL cells after treatment with 1.25 μM of STF-62247 or doxorubicin for 24 hours. All error bars represent the SEM. Scale bar, 10 μm.

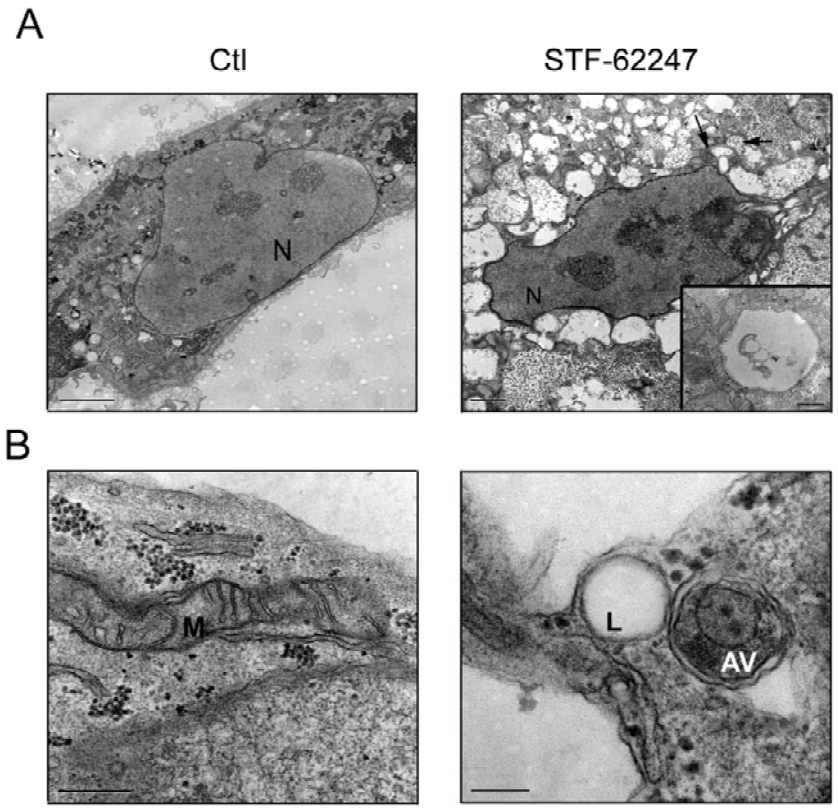

Figure S2.

(A) Transmission electron microscopy in RCC4 cells treated with vehicle control (DMSO) or with 1.25 μM STF-62247 for 20 hrs. Arrows represent autophagic vacuoles during drug treatment. N. Nucleus. Scale bar on the left panel, 5 μm. Scale bar on the right panel, 2 μm and 0.5 μm (insert).

(B) RCC4 cells treated with STF-62247 observed at higher magnification. M. Mitochondria L. Lysosome AV. Autophagic Vacuole. Scale bar on the left panel, 0.5 μm and on the right panel, 0.2 μm.

Figure S3

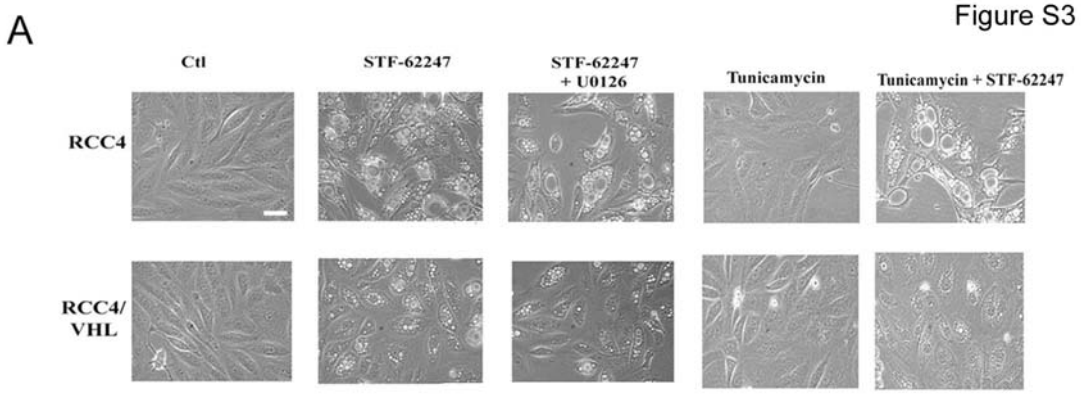
A
Ctl
STF-62247
STF-62247 + U0126
Tunicamycin
Tunicamycin + STF-62247
RCC4
RCC4/ VHL

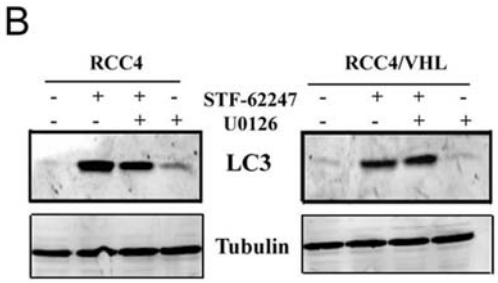
B
RCC4
RCC4/VHL
STF-62247
U0126
LC3
Tubulin

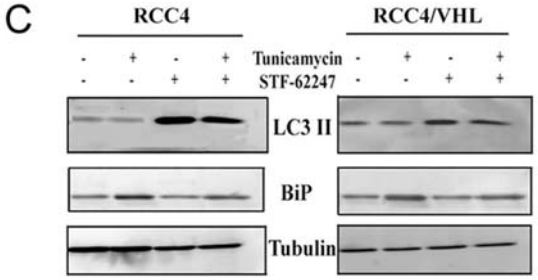
C
RCC4
RCC4/VHL
Tunicamycin
STF-62247
LC3 II
BiP
Tubulin

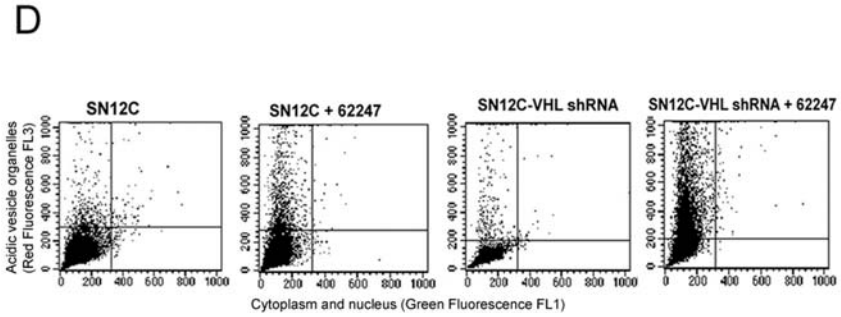
D
SN12C
SN12C + 62247
SN12C-VHL shRNA
SN12C-VHL shRNA + 62247
Acidic vesicle organelles (Red Fluorescence FL3)
Cytoplasm and nucleus (Green Fluorescence FL1)

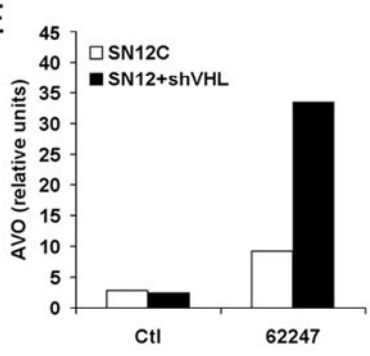
E
SN12C
SN12+shVHL
AVO (relative units)
Ctl
62247

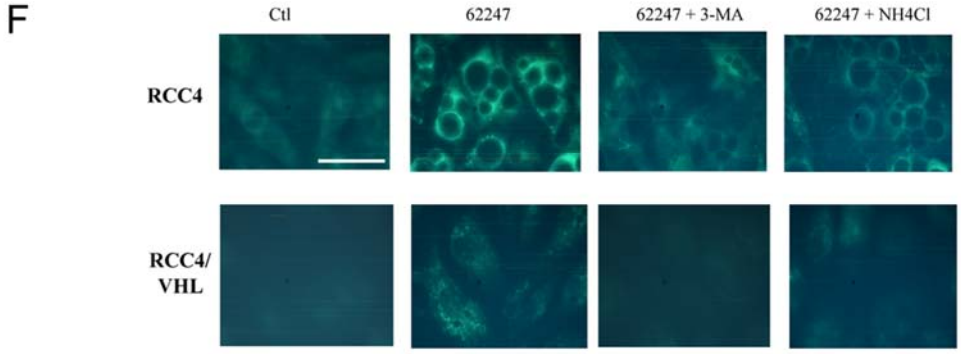
F
Ctl
62247
62247 + 3-MA
62247 + NH4Cl
RCC4
RCC4/ VHL

Figure S3.

(A) VHL-deficient RCC4 and wild-type VHL were incubated in presence of 10 μM U0126, or 2 μg/ml tunicamycin with 1.25 μM of STF-62247 for 20 hrs and the presence of vacuoles was examined under light microscopy.

(B and C) LC3 processing was evaluated by Western blot after the treatment with U0126 or tunicamycin in presence or absence of STF-62247 as described above. Tubulin was used as loading control.

(D) FACS analysis to measure the acidic vesicle organelles after staining with acridine orange in SN12C and SN12C-VHL shRNA following treatment with STF-62247 for 24 hours.

(E) AVO quantification from the FACS analysis in A.

(F) Autophagic vacuoles stained with MDC. After STF-62247 treatment with or without 3-MA, NH_4Cl, MDC was added the last 10 minutes. Then, cells were fixed, washed with PBS and observed directly under microscope. Scale bar, 10 μm.

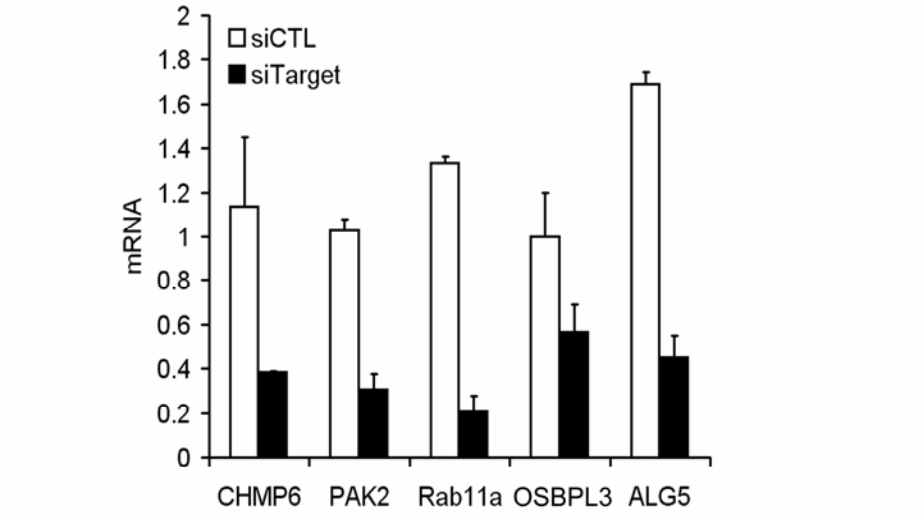

Figure S4. qRT-PCR Analysis to Examine Knockdown of a Given Target Gene by siRNA Transfection